Proposed material release plan for the decommissioning of the ESRF storage ring

P. Berkvens, P. Colomp

ESRF, 38043 Grenoble Cedex 9, France

Abstract

The ESRF Council has approved the ESRF Phase II Upgrade, including a major upgrade of the storage ring. The installation of the new storage ring, in the existing tunnel, will require the dismantling of almost all components of the existing storage ring. Following discussions with the French Nuclear Safety Authority, ESRF has carried out detailed activation calculations and has proposed a material release plan. The present papers describes the main points of this plan.

1. Introduction

Article L542-1-1 of the French Environmental Act [1] gives the following definition of radioactive waste:
*"*A radioactive material is a material containing radionuclides, natural or artificial, whose activity or concentration justify radiation protection control measures. Radioactive waste is a radioactive material for which no further use is foreseen or envisaged.*"*
The French radiation protection legal framework does not define formal clearance levels for the reuse, recycling or conventional disposal of materials.
The planned decommissioning of the ESRF storage ring will produce a large quantity of accelerator components with no further use for the ESRF: more than 600 magnets (approximately 500 tons of steel and 80 tons of copper), more than 400 vacuum vessels (approximately 10 tons of stainless steel), of the order of 200 supports, a large number of cable trays and several km of cables.
Only a limited number among these accelerator components will be radioactive, according to the definition given above. The radioactivity and radioactivity concentrations in the majority of the dismantled accelerator components will indeed be such that the potential dose impact to the general public and to the environment due to the release of these materials is completely negligible and would not justify any further radiation protection control measures. ESRF therefore hopes that the latter accelerator components could be cleared for reuse, recycling or conventional disposal.
Discussions between the French Nuclear Safety Authority (*ASN, Autorité de Sûreté Nucléaire*) and the ESRF have been undertaken on this subject. It was finally agreed that ESRF should submit to the ASN a detailed technical report describing the activation of the storage ring and proposing a methodology for the possible clearance of certain accelerator components.

2. Proposed Clearance Criterion

The fundamental criterion that ESRF proposes for the clearance of materials for reuse, recycling or conventional disposal is the requirement for the corresponding surface dose rates to be

indistinguishable from background (1)

Clear measurement protocols should guarantee the "indistinguishable from background" criterion. These protocols will be based on the use of very sensitive instruments to obtain very low decision thresholds and detection limits. These low limits will guarantee that the potential dose impact to the general public and to the environment due to the release of the materials is negligible.
In parallel, we've verified that this criterion also guarantees the compliance with the clearance levels defined in the Council Directive 2013/59/EURATOM [2]. For a given accelerator component, with SE_i the activity concentration value for the i^{th} isotope present in the accelerator component, as defined in Table A, Part 1 of Annex VII of the 2013/59/EURATOM Directive, and with AS_i the specific activity of the corresponding isotope, the sum over all isotopes of the fractions of the specific activity to the corresponding activity concentration value shall not exceed one:

$$\sum_{all\ isotopes} \frac{AS_i}{SE_i} \leq 1 \quad (2)$$

Table 1 shows the clearance levels defined in the 2013/59/EURATOM Directive for the most important isotopes in the frame of the induced radioactivity of the ESRF storage ring components.

H^3	Cr^{51}	Mn^{52}	Mn^{54}	Fe^{55}	Co^{56}	Co^{57}	Co^{58}	Co^{60}	Ni^{63}
100	100	1	0.1	1000	0.1	1	1	0.1	100

Table 1 - Clearance levels (Bq/g) defined in the 2013/59/EURATOM Directive for the most important isotopes in the frame of the induced radioactivity of the ESRF storage ring components.

3. Process Knowledge

The decision of whether a given accelerator component can be cleared for reuse, recycling or conventional disposal will in fine depend on the results of radiation measurements, following clearly defined measurement protocols, which must guarantee the formal clearance criterion. Process knowledge however is very important because it will e.g. allow a graded approach when defining the measurement protocols, using information concerning a possible zoning inside the storage ring tunnel in terms of induced radioactivity. Knowledge about the physical processes of radioisotope production will help understand why such a zoning is indeed possible. It will also help us in choosing the right radiation monitors, capable of measuring the radioisotopes we must detect, etc.
The following process knowledge is mandatory to allow the correct evaluation of induced radioactivity in the ESRF storage ring:

- The physical processes involved in the production of radioisotopes and knowledge of the radioactive decay of the produced radioisotopes,
- The characteristics of the storage ring, including general layout, beam optics information and detailed knowledge of the different accelerator components (geometry, material composition, etc.),
- Operational information of the accelerator facility, including operational cycles, beam loss patterns, etc.

3.1 Beam Losses

Knowledge of the beam loss power is a key parameter in the evaluation of the induced radioactivity in the storage ring. Values for the beam loss power can be obtained from the total number of electrons injected in the storage ring and from the way these electrons are subsequently lost along the storage ring. Detailed knowledge of both processes is available at the ESRF.
When studying activation of the storage ring components in view of their decommissioning, the time structure of the electron losses can be obtained directly from the time structure of the injected electron charge in the storage ring. Indeed, the lifetime of the electrons, i.e. the time between their injection and their final loss, responsible for the activation, will be at maximum a few days and on average a few hours, while we are looking at isotopes with decay constants of hundreds of days. The electron charge injected in the ESRF storage ring is continuously measured using a beam current monitor installed at the end of the transfer line between the booster synchrotron and the storage ring. Figure 1 shows the cumulative injected electron charge for the period from 01/05/1998 to 31/12/2014.
Inside the ESRF storage ring, a beam loss monitoring system, based on PTW T7262 50 liter ionisation chambers, is installed. One ionisation chamber per unit cell is installed. These very sensitive ionisation chambers, shielded with 1 cm of lead against scattered synchrotron radiation, allow determining local beam losses via the measurement of scattered bremsstrahlung.
These monitors allow an accurate determination of the percentage of the total electron losses that occur in each of the 32 unit cells of the storage ring. The results show that 70 to 80 % of the beam losses are concentrated in two special sections (injection cell and scraper), whereas the local beam losses in the majority of the standard unit cells account for 1 % or less of the total beam losses.
Within a standard unit cell, the initiating electron losses occur essentially on the input tapers of the straight section insertion device vacuum chamber or on the input tapers of the in-vacuum undulators. For all calculations so far we have therefore assumed the losses to occur on these tapers (electrons were assumed to hit the taper with zero angle and with a uniform distribution from 0 to 50 μm from the edge of the taper). The

ESRF beam dynamics group are presently doing sophisticated beam loss calculations to provide more detailed loss patterns within the unit cells. Although we expect little effect on the induced radioactivity maps, the latter will be redone for the final simulations prior to the dismantling, using these more detailed loss patterns.

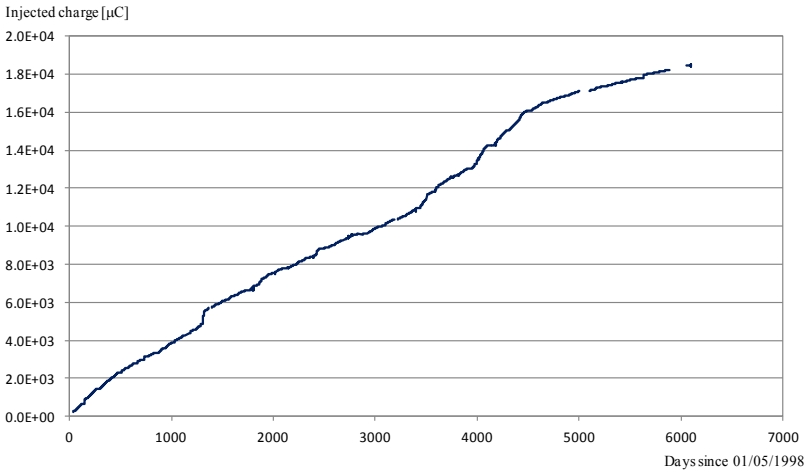

Fig.1 – Cumulative injected electron charge in the storage ring during the period 01/05/1998 to 31/12/2014.

In conclusion, the combined knowledge of the injected electron charge and the readings of the 32 beam loss ionisation chambers allow us to know precisely the absolute beam losses in each of the 32 unit cells. As all these data are recorded in the ESRF accelerator database, we can reconstruct the beam loss history at any point in time, in particular we will be able to reconstruct the beam loss history at the time of the final shutdown of the storage ring prior to its dismantling.

4. FLUKA model

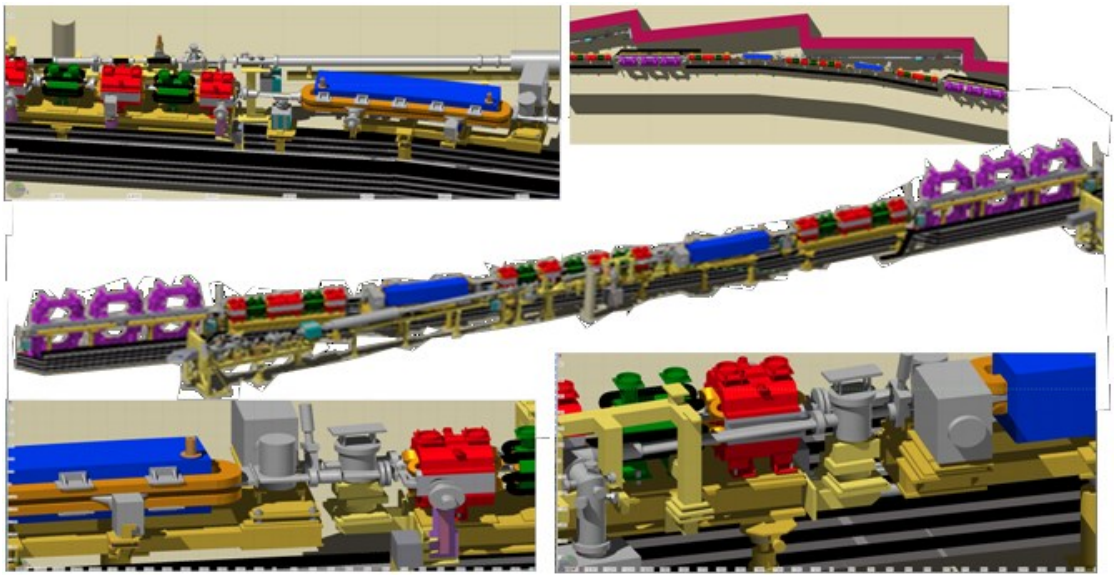

Fig.2 – FLUKA model of the storage ring.

We have built a detailed FLUKA [3] model of the ESRF storage ring, based on the manufacturing drawings of the magnets, vacuum vessels, supports etc. Figure 2 illustrates this model.
The magnetic fields of the dipole magnets, quadrupole magnets and sextupole magnets were integrated in the model (analytical hard-edge description). The accuracy of the magnetic lattice has been verified by different ray tracing calculations for on- and off-momentum electrons, as well as on- and off-axis electrons.
The materials of the different components were obtained from the manufacturing drawings. However they don't mention the exact compositions. As a conservative approach, we have used for each of the different alloys the maximum concentrations for all constituents, other than the main one, as specified by the

corresponding standards. In this way the induced specific activities of the major isotopes will be maximised (this approach will marginally reduce the Fe^{55} specific activity in the different steels, but the contribution of Fe^{55} is negligible both in terms of residual surface dose rates and with respect to the clearance levels of the European Directive).

5. Indistinguishable From Background Criterion

As mentioned earlier, the fundamental criterion for the clearance of materials is the requirement that the corresponding surface dose rates must be indistinguishable from background. We translate this general principle in practical criteria to be used in the corresponding measurement protocols.
We base the determination of the minimum detectable count rate on the French NF ISO 11929 standard from May 2010 [4] concerning the determination of the characteristic limits (decision threshold, detection limit and limits of the confidence interval) for measurements of ionizing radiation.

The choice of the radiation detector to be used with the measurement protocol will be a compromise between two criteria

1. The compactness of the detector, to allow carrying out count rate measurements close to the surface of the accelerator components, e.g. on the surface of the quadrupole and sextupole pole tips, where the induced radioactivity is the highest.
2. A sufficiently large active volume of the detector to obtain sufficiently large count rates, necessary to obtain a sufficiently low detection limit, to meet the "indistinguishable from background criterion" while keeping the duration of the measurements to a reasonable value.

Most standard survey counters fulfil the 1st criterion, but have typical background count rates of the order of 1 count per second or less. Assuming a typical background dose rate of 30 $nSv \cdot h^{-1}$, even for an unreasonably long measurement time of 30 minutes the detection limit (6.1 $nSv \cdot h^{-1}$) would still be too high to meet the clearance criteria.
The use of a standard survey monitor will therefore not allow defining a practical measurement protocol with a sufficiently low detection limit.
At the other end of the range of radiation detectors are the very-large-size scintillator counters and the high-purity Ge-detectors. While these detectors certainly fulfil the 2nd criterion mentioned above, they do not allow, due to their size or the complexity of the instrument, to carry out surface count rate measurements for many of the complex geometries found in the accelerator components, particularly in the case of quadrupole and sextupole magnets.
Only a few, sophisticated radiation monitors will fulfil simultaneously both criteria. These monitors are relatively compact, handheld monitors using typically scintillator detectors with a relatively large volume. One of these monitors is the Exploranium Gr-130 miniSPEC detector, using a 1.5" × 1.5"× 2" (3.8 cm × 3.8 cm × 5.1 cm) NaI(Tl) scintillator. The detector has a count rate of 1.37 count per second per $nSv \cdot h^{-1}$, corresponding to a count rate of 41 counts per second for a typical background of 30 $nSv \cdot h^{-1}$. Furthermore, the monitor allows averaging the count rate for measurement durations between 1 and 60 seconds.
Using a measurement time of 1 minute, we obtain the following values for the decision threshold and the detection limit (for a typical background of 30 $nSv \cdot h^{-1}$):

Decision threshold: 3.62 counts per second (3)
Detection limit: 7.40 counts per second (4)

Apart from the count rate measurement, the Gr-130 miniSPEC detector has a dose monitor mode, providing dose rates expressed in air kerma free-in-air. Concerning the calibration, the user manual [5] mentions that *"the sodium-iodide detector gives highly accurate dose levels, which are essentially flat across the entire energy spectrum; calibration data show less than 1 % error across the entire spectrum.···The system calibration was verified at the IAEA certified Seibersdorf National Laboratory in Austria. The certification process was actually tested from 60 keV to 3000 keV."*
We have carried out a number of count rate measurements and dose rate measurements using different calibration sources to verify that, when indeed assuming a flat calibration curve in terms of air kerma, we obtain consistent results and to finally obtain a conversion factor between count rate and ambient dose equivalent rate. We obtain the following values for the decision threshold and detection limit expressed in ambient dose equivalent (for a typical background level of 30 $nSv \cdot h^{-1}$):

Decision threshold: 3.62 counts per second or 2.68 nSv·h^{-1} (5)
Detection limit: 7.40 counts per second or (6)
Stainless steel: 4.54 nSv·h^{-1} (7)
Magnet yokes: 5.78 nSv·h^{-1} (8)

In conclusion, we have demonstrated that when using the Gr-130 miniSPEC detector and with measurement times of 1 minute, we obtain very small values for both the decision threshold and the detection limit which will allow the definition of a measurement protocol based on the "indistinguishable from background" criterion. It is worth recalling that these values are much smaller than what can be obtained with any conventional survey monitor.

6. Results from Calculations

3D activation maps have been calculated for all the different storage ring components. An example is shown in figure 3. The results show that for the standard cells, all components (magnets, vacuum vessels, supports, …) should meet the indistinguishable from background clearance criterion, with possibly the need of a few years cooling down for some specific vacuum vessels.

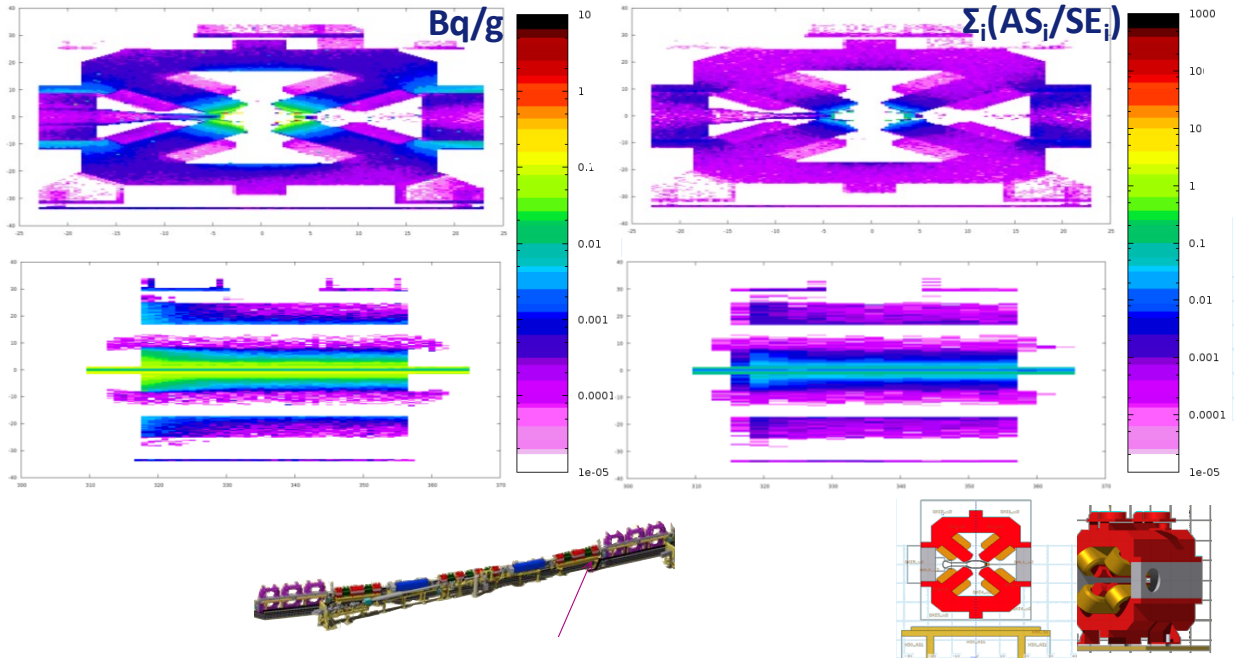

Fig.3 – Activation results for quadrupole Q1. Left: total specific activity (all isotopes). Right: sum specific activities/clearance levels (all isotopes). Top: integrated over all z; bottom: integrated over x = [2.6 – 3.8 cm]. Annual beam losses: 400 μC, 1 % local losses, 1 month cooling time.

7. Minimum Detectable Specific Activity

We have shown how surface count rate measurements using very sensitive equipment such as the Gr-130 miniSPEC detector can be used to guarantee the fundamental indistinguishable from background criterion for the clearance of material. We can demonstrate that the respect of the indistinguishable from background criterion will automatically guarantee the respect of the relation (2) concerning the Council Directive 2013/59/EURATOM clearance levels.
The 2013/59/EURATOM Directive does not specify the minimum volume for which the relation (2) must hold. In a very restrictive and conservative manner, we will guarantee relation (2) in any 1 cm^3 cube. In this way we deal with the possible presence of hotspots inside the accelerator component. The sum of fractions in (2) is almost exclusively determined by the specific activity of Mn^{54}, with a clearance level SE_{Mn54} = 0.1 Bq·g^{-1}. With a density for steel of 8 g·cm^{-3}, respecting expression (2) means that we are tracking down hotspots with Mn^{54} activities of 1 Bq or less! It is obvious that further reducing this scoring volume doesn't

make any sense. As a consequence, when dealing with vacuum vessels, with wall thicknesses typically much smaller than 1 cm, we will adapt the shape of the scoring volume to keep its 1 cm^3 volume.
Extensive calculations concerning the detection thresholds for volumetric radioactivity using surface survey detection techniques have been conducted at SLAC [6]. They mention a typical ratio of the surface dose rate at 2 cm and the activity of the proxy radioisotopes of 10 $nSv \cdot h^{-1}$ per 37 $mBq \cdot g^{-1}$ (1 $\mu rem \cdot h^{-1}$ per 1 $pCi \cdot g^{-1}$). Their calculations also show that if the activation depth is smaller than 2 cm, the sensitivity drops significantly (when expressing the sensitivity as a function of the specific activity within the narrow depth volume). These results indicate that in the case of uniform volumetric activation of bulky material, the detection limits obtained above will be largely sufficient to verify the relation (2), since in our case the main proxy-isotope is Mn^{54}, with a clearance level SE_i = 100 $mBq \cdot g^{-1}$. However, since we are dealing almost exclusively with geometries where the activation extends over a small depth in the accelerator component, as is the case in the pole tips of the quadrupoles and sextupoles, or where the activation concerns small thickness components, as is the case of vacuum vessels, we examined all specific geometries using the FLUKA code. An example is shown in figure 4, for a quadrupole magnet, where the highest specific activation is situated on the pole tips. For this geometry, with our detection limit of 5.78 $nSv \cdot h^{-1}$ (see expression 8) we will be able to detect 1 cm^3 hotspots with a value for the sum of fractions $\sum_i (AS/SE)_i \geq 0.67$. We obtained similar results for all other geometries.

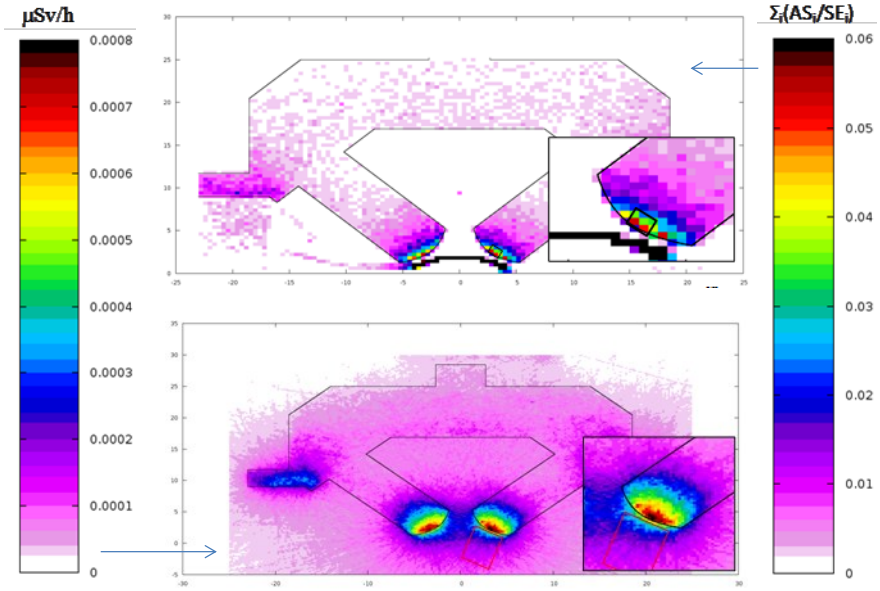

Fig.4 – Top: sum of fractions $\sum_i (AS/SE)_i$, in quadrupole Q1, averaged over the first 6 cm from the entrance face of the yoke. Bottom: residual ambient dose equivalent rates around the upper half yoke of quadrupole Q1, averaged over the first 6 cm from the entrance face of the yoke. Annual beam losses: 400 µC, 1 % local losses, 1 month cooling time.

References

[1] Code de l'Environnement, http://www.legifrance.gouv.fr/
[2] Council Directive 2013/59/Euratom of 5 December 2013, laying down basic safety standards for the protection against the dangers arising from exposure to ionising radiation, Official Journal of the European Union, L13/1 – L13/73, 17 January 2014
[3] A. Fassò et al., FLUKA: a Multi-Particle Transport Code, CERN-2005-10,INFN/TC_05/11, SLAC-R-773,2005
[4] French standard NF ISO 11929 concerning the determination of the characteristic limits (decision threshold, detection limit and limits of the confidence interval) for measurements of ionizing radiation, Association Française de Normalisation (AFNOR — French standard institute), 1st issue 2010-05-P, May 2010
[5] GR-130 miniSPEC User Manual, http://www.qsl.net/k/k0ff/Exploranium/130manual rev15.1.pdf
[6] SLAC Material Release Program Manual, RP Department Document RPD-010, Revision 0, SLAC-I-760-2A-05C-024, Stanford Linear Accelerator Center, 09/02/2011